A Novel Nonlinear Approach to Suppress Resonant Vibrations

Bin Zhang[a], Stephen A. Billings[a] , Zi-Qiang Lang[a], and Geofrey R. Tomlinson[b]

[a]*Department of Automatic Control and Systems Engineering, The University of Sheffield, Mappin Street, Sheffield S1 3JD, UK*
[b]*Department of Mechanical Engineering, The University of Sheffield, Mappin Street, Sheffield S1 3JD, UK*

Dept of Automatic Control and Systems Engineering
The University of Sheffield, Sheffield, S1 3JD, UK

Research Report No. 951

May 2007

A Novel Nonlinear Approach to Suppress Resonant Vibrations

Bin Zhang[a], Stephen A. Billings[a] , Zi-Qiang Lang[a], and Geofrey R. Tomlinson[b]

[a]*Department of Automatic Control and Systems Engineering, The University of Sheffield, Mappin Street, Sheffield S1 3JD, UK*
[b]*Department of Mechanical Engineering, The University of Sheffield, Mappin Street, Sheffield S1 3JD, UK*
E-mail: {Bin.Zhang, S.Billings, Z.Lang, g.tomlinson}@sheffield.ac.uk

Abstract

A novel approach to suppress resonant vibration is presented by employing a single degree of freedom transmissibility system which utilizes a nonlinear damping element. Studies have shown that the nonlinear damping element can reduce the output energy at the driving frequency and at the same time spread the output signal energy over a wider range of harmonics. It will also be shown that the reduction becomes larger as the nonlinear damping characteristic gets stronger and in most cases, the power at the harmonics in the output spectrum will be much less if the nonlinear damping characteristic is an odd function. Hence, an odd polynomial nonlinear damping element can be introduced between the incoming signal and the structure of interest to suppress resonant vibration. An expression is derived to express the transmitted force spectrum in terms of the nonlinear generalized frequency response functions, to clearly show how the energy, at the excitation frequency, is modified by the nonlinearity.

Keywords: energy transfer; damping; vibration transmissibility; nonlinear materials; higher-order frequency response functions

1. Introduction

Resonance is a well-known phenomenon in engineering, which arises when the excitation frequency at an operating condition is near a natural frequency of the system. When a resonance occurs for a system, the resulting vibration levels can be very high and this can cause considerable damage. Suppressing resonant vibration is therefore very important to ensure an appropriate running condition and a desired behaviour of the system [1-4]. The standard approach to suppress resonant vibration is to either introduce damping or a vibration absorber which can be passive, active or a combined approach [5, 6].

This paper describes an entirely different approach which results in a novel way of avoiding resonant vibration. The concept is to transfer or distribute the incoming energy in such a way that the energy entering the resonant region of the structure of interest is reduced to a level which avoids significant problems by introducing a non-linearity between the input and the structure. A analytic relationship between the system output frequency response and the non-linearity is derived in this study to

reveal how the energy entering the structure is modified by the non-linearity, which results in energy transfer.

2. System description

In order to explain the concept of energy transfer in an analytical sense, the effect of introducing a nonlinear element (in this case a nonlinear damper) at the interface between the input of a single degree of freedom (SDOF) system and the output will be studied.

Consider the SDOF system shown in Fig. 1. This represents a mass supported on a linear elastic spring k in parallel with a nonlinear damper $f(\cdot)$. The mass is subjected to a harmonic excitation force of amplitude F_d and frequency Ω and the output of interest is the force $F_s(t)$ transmitted to the support via the linear spring and the nonlinear damper.

The nonlinear damping element is described by a polynomial function of velocity such that

$$f(\cdot) = a_1(\cdot) + a_3(\cdot)^3 \tag{1}$$

where a_1, a_3 are the parameters of the damping characteristic and a_3 represents the system nonlinearity.

The equilibrium equation for the system in Fig. 1 and corresponding force at the support can be expressed as

$$m\ddot{x}(t) + a_1\dot{x}(t) + a_3\dot{x}^3(t) + kx(t) = F_d\cos(\Omega t) \tag{2}$$

$$F_s(t) = a_1\dot{x}(t) + a_3\dot{x}^3(t) + kx(t) \tag{3}$$

For convenience of analysis, denote

$$y_d(t) = x(t) \tag{4}$$

$$y_F(t) = F_s(t) \tag{5}$$

and

$$u(t) = F_d\cos(\Omega t) \tag{6}$$

The system can then be described by a single input two output system

$$m\ddot{y}_d(t) + a_1\dot{y}_d(t) + a_3\dot{y}_d{}^3(t) + ky_d(t) = u(t) \tag{7}$$

$$y_F(t) = a_1\dot{y}_d(t) + a_3\dot{y}_d{}^3(t) + ky_d(t) \tag{8}$$

What is of interest in this study is how the spectrum of the transmitted force $2\left|Y_F\left(j\Omega\right)\right|$ depends on the nonlinear damping element which in turn creates harmonics that spread the incoming energy to other frequencies, resulting in a reduction in the transmitted force level of $2\left|Y_F\left(j\Omega\right)\right|$ at the excitation frequency Ω.

Notice that $2\left|Y_F\left(j\Omega\right)\right|$ not $\left|Y_F\left(j\Omega\right)\right|$ is used because $2\left|Y_F\left(j\Omega\right)\right|$ represents the physical magnitude of the system output $y_F\left(t\right)$ at the frequency Ω.

3. Volterra modelling of the system in the time and frequency domain

The output $y\left(t\right)$ of a single input single output (SISO) analytical system can be expressed as a Volterra functional polynomial of the input $u\left(t\right)$ to give

$$y\left(t\right)=\sum_{\mathrm{n=1}}^{\mathrm{N}}\mathrm{y}^{(\mathrm{n})}\left(t\right)$$

(9)

where N is the maximum order of the system nonlinearity and $y^{(n)}\left(t\right)$ is the nth-order output of the system, which is given by

$$y^{(n)}\left(t\right)=\int_{-\infty}^{+\infty}\cdots\int_{-\infty}^{+\infty}h_n\left(\tau_1,\cdots,\tau_n\right)\prod_{i=1}^{n}u\left(t-\tau_i\right)d\tau_i \qquad n\geq 1$$

(10)

where $h_n\left(\tau_1,\cdots,\tau_n\right)$ is a real valued function of $\tau_1,\cdots,\tau_n$ called the nth order impulse response function or Volterra kernel of the system [7, 8]. Volterra generalised the linear convolution concept to deal with nonlinear systems by replacing the single impulse response with a series of multidimensional integration kernels. The nth-order Volterra kernel describes nonlinear interactions among n copies of the input. The multidimensional Fourier transform of the nth-order Volterra kernel yields the nth-order transfer function or generalised frequency response function (GFRF)

$$H_n\left(j\omega_1,\cdots,j\omega_n\right)=\int_{-\infty}^{+\infty}\cdots\int_{-\infty}^{+\infty}h_n\left(\tau_1,\cdots,\tau_n\right)e^{-j\left(\omega_1\tau_1+\cdots+\omega_n\tau_n\right)}d\tau_1\cdots d\tau_n$$

(11)

Using the concept of GFRF, the general relationship between the input spectrum $U\left(j\omega\right)$ and the output spectrum $Y\left(j\omega\right)$ can be obtained as [9]

$$Y\left(j\omega\right)=\sum_{n=1}^{N}\frac{1}{\sqrt{n}\left(2\pi\right)^{n-1}}\int_{\omega_1+\cdots+\omega_n=\omega}H_n\left(j\omega_1,\cdots,j\omega_n\right)\prod_{i=1}^{n}U\left(j\omega_i\right)d\sigma_{\omega n}$$

(12)

where $\int_{\omega_1+\cdots+\omega_n=\omega}\left(\cdot\right)d\sigma_{\omega n}$ denotes the integration of $\left(\cdot\right)$ over the n-dimensional hyperplane $\omega_1+\cdots+\omega_n=\omega$.

When the system is subject to a multi-tone input such as

$$u(t)=\sum_{i=1}^{K}|A_i|\cos(\omega_i t+\angle A_i)$$

(13)

Lang and Billings [9] showed that Eq. (12) can be expressed as

$$Y(j\omega)=\sum_{n=1}^{N}\frac{1}{2^n}\sum_{\omega_{k_1}+\cdots+\omega_{k_n}=\omega}H_n(j\omega_{k_1},\cdots,j\omega_{k_n})A(\omega_{k_1})\cdots A(\omega_{k_n})$$

(14)

where

$$k_l\in\{-K,\cdots,-1,1,\cdots,K\},\quad l=1,\cdots,n,$$

$$A(\omega)=\begin{cases}|A_k|e^{j\angle A_k} & if\quad \omega\in\{\omega_k,k=\pm1,\cdots,\pm K\}\\ 0 & otherwise\end{cases},$$

$$\omega_{-k}=-\omega_k$$

and

$$|A_{-k}|e^{j\angle A_{-k}}=|A_k|e^{-j\angle A_k}$$

In our case, we have a single input, the force excitation, and two outputs, the displacement of the mass m and the force transmitted to the support. Eq. (14) now takes the form [10, 11]

$$Y_{j_1}(j\omega)=\sum_{n=1}^{N}\frac{1}{2^n}\sum_{\omega_{k_1}+\cdots+\omega_{k_n}=\omega}H_{nj_1}(j\omega_{k_1},\cdots,j\omega_{k_n})A(\omega_{k_1})\cdots A(\omega_{k_n})\qquad j_1=1,2$$

(15)

where

$$H_{nj_1}(j\omega_1,\cdots,j\omega_n)=\int_{-\infty}^{+\infty}\cdots\int_{-\infty}^{+\infty}h_{nj_1}(\tau_1,\cdots,\tau_n)e^{-j(\omega_1\tau_1+\cdots+\omega_n\tau_n)}d\tau_1\cdots d\tau_n$$

is the nth order GFRF of the system corresponding to the j_1th output and

$$k_l\in\{-1,+1\},\quad l=1,\cdots,n,$$

$$A(\omega)=\begin{cases}|A_k|e^{j\angle A_k} & if\quad \omega\in\{\omega_k,k=\pm1\}\\ 0 & otherwise\end{cases},$$

where $|A_{\pm1}|=F_d$, $\omega_{\pm1}=\pm\Omega$, $\angle A_{\pm1}=0$.

4. The effects of system nonlinearity on the output frequency response

The focus of this section is to investigate the effects of the nonlinear damping characteristic of the systems (2) and (3) on the output frequency response when the system is subject to a multi-tone or a harmonic input. This study involves two steps. First the GFRF matrices of the system

$$\left[H_{nd}(j\omega_1,\cdots,j\omega_R),\quad H_{nF}(j\omega_1,\cdots,j\omega_R)\right],\quad \text{n=1,2,3,}\cdots$$

are derived. Then a relationship between the system output frequency response $Y_F(j\omega)$ and the system GFRFs is determined.

4.1 The probing method

Given a parametric model of a nonlinear system, there are a number of methods to obtain the GFRFs of the system. Arguably the most direct is the harmonic probing method of Bedrosian and Rice [12] and Bussgang et al [13]. In the case of single input single output nonlinear systems, the basic idea of the probing method can be introduced as below.

It was shown by Rugh [14] that for nonlinear systems which are described by the Volterra model (9), (10) and excited by a combination of exponentials

$$u(t)=\sum_{i=1}^{R} e^{j\omega_i t} \quad , \qquad 1 \le R \le N$$

(16)

the output response can be written as

$$\begin{aligned} y(t) &= \sum_{n=1}^{N}\sum_{i_1=1}^{R}\cdots\sum_{i_n=1}^{R} H_n\left(j\omega_{i_1},\cdots,j\omega_{i_n}\right) e^{j\left(\omega_{i_1}+\cdots+\omega_{i_n}\right)t} \\ &= \sum_{n=1}^{N}\sum_{m(n)} G_{m_1(n)\cdots m_R(n)}\left(j\omega_1,\cdots,j\omega_R\right) e^{j\left[m_1(n)\omega_1+\cdots+m_R(n)\omega_R\right]t} \end{aligned}$$

(17)

where $\sum_{m(n)}$ indicates a R-fold sum over all integer indices $m_1(n),\cdots,m_R(n)$ such that $0 \le m_i(n) \le n$, $m_1(n)+\cdots+m_R(n)=n$, and

$$G_{m_1(n)\cdots m_R(n)}\left(j\omega_1,\cdots,j\omega_R\right)=\frac{n!}{m_1(n)!\cdots m_R(n)!}H_n\left(\underbrace{j\omega_1,\cdots,j\omega_1}_{m_1(n)},\cdots,\underbrace{j\omega_R,\cdots,j\omega_R}_{m_R(n)}\right)$$

(18)

Notice that in Eq. (18) when $n=R$, $m_i(n)=1$, $i=1,\cdots,R$, therefore

$$G_{m_1(R)\cdots m_R(R)}\left(j\omega_1,\cdots,j\omega_R\right)=R!H_R\left(j\omega_1,\cdots,j\omega_R\right)$$

(19)

Considering Eq. (19), Eq. (17) can be written as

$$\begin{aligned} y(t) = &\sum_{n=1,n\neq R}^{N}\sum_{m(n)} G_{m_1(n)\cdots m_R(n)}\left(j\omega_1,\cdots,j\omega_R\right) e^{j\left[m_1(n)\omega_1+\cdots+m_R(n)\omega_R\right]t} \\ &+R!H_R\left(j\omega_1,\cdots,j\omega_R\right)e^{j(\omega_1+\cdots+\omega_R)t} \end{aligned}$$

(20)

For nonlinear systems which have a parametric model with parameter vector θ,

$$y(t)=f_0\left(t,\theta,y(t),u(t)\right)$$

(21)

and which can also be described by the Volterra model (9) and (10), substituting Eqs. (16) and (20) into Eq. (21) for y(t) and u(t), and extracting the coefficient of $e^{j(\omega_1+\cdots+\omega_R)t}$ from the resulting expression produces an equation from which the GFRF $H_R\left(j\omega_1,\cdots,j\omega_R\right)$ can be obtained.

If the system is of a single input and two outputs and can be described by the parametric model

$$\begin{cases} y_1(t) = f_1\left(t,\theta, y_1(t), y_2(t), u_1(t)\right) \\ y_2(t) = f_2\left(t,\theta, y_1(t), y_2(t), u_1(t)\right) \end{cases},$$

(22)

Eq. (20) can be written as

$$y_{j_1}(t) = \sum_{n=1, n\neq R}^{N} \sum_{m(n)} G_{m_1(n)\cdots m_R(n) j_1}\left(j\omega_1, \cdots, j\omega_R\right) e^{j\left[m_1(n)\omega_1 + \cdots + m_R(n)\omega_R\right]t} + R! H_{Rj_1}\left(j\omega_1, \cdots, j\omega_R\right) e^{j(\omega_1 + \cdots + \omega_R)t} \qquad j_1 = 1, 2$$

(23)

where

$$G_{m_1(n)\cdots m_R(n) j_1}\left(j\omega_1, \cdots, j\omega_R\right) = \frac{n!}{m_1(n)! \cdots m_R(n)!} H_{nj_1}\left(\underbrace{j\omega_1, \cdots, j\omega_1}_{m_1(n)}, \cdots, \underbrace{j\omega_R, \cdots, j\omega_R}_{m_R(n)}\right).$$

(24)

Then substituting $u_1(t) = \sum_{i=1}^{R} e^{j\omega_i t}$, and $y_1(t)$ and $y_2(t)$ given by Eq. (23) into Eq. (22), and extracting the coefficient of $e^{j(\omega_1 + \cdots + \omega_R)t}$ from the resulting expressions produces two coupled equations for which the GFRF matrix

$$\left[H_{Rd}\left(j\omega_1, \cdots, j\omega_R\right), \quad H_{RF}\left(j\omega_1, \cdots, j\omega_R\right)\right]$$

can be obtained.

4.2 Derivation of the system GFRFs

4.2.1 Derivation of the GFRFs for $y_d(t)$

The expression for $H_{nd}\left(j\omega_1, \cdots, j\omega_n\right)$ was derived by Zhang et al [15] and will simply be quoted here.

When $n = 1$,

$$H_{1d}\left(\omega_1\right) = \frac{1}{\beta\left(j\omega_1\right)}$$

(25)

When n is an even number, $H_{nd}\left(\omega_1, \cdots, \omega_n\right) = 0$.

When $n \geq 3$ and is an odd number,

$$H_{nd} = 3! a_3 c_n^{1-n} M^{(3)}$$

(26)

where

$$c_n^{1\cdots n} = -\frac{1}{\beta\left(j\omega_1 + \cdots + j\omega_n\right)} \times \frac{1}{n!}$$

(27)

$$\beta\left(j\sum_{i=1}^{n}\omega_i\right) = m\left(j\sum_{i=1}^{n}\omega_i\right)^2 + a_1\left(j\sum_{i=1}^{n}\omega_i\right) + k$$

(28)

$$M^{(3)} = \sum_{(r;3,n)}{\sum_N}' r_1!\left(j\omega_1 + \cdots + j\omega_{r_1}\right)H_{r_1}\left(\omega_1,\cdots,\omega_{r_1}\right)r_2!\left(j\omega_{r_1+1} + \cdots + j\omega_{r_1+r_2}\right)H_{r_2}\left(\omega_{r_1+1},\cdots,\omega_{r_1+r_2}\right)$$

$$r_3!\left(j\omega_{r_1+r_2+1} + \cdots + j\omega_n\right)H_{r_3}\left(\omega_{r_1+r_2+1},\cdots,\omega_n\right)$$

(29)

Formally,

$$M^{(3)} \triangleq \sum_{p=1}^{\left|S_n^3\right|} S_n^3[p]$$

(30)

where S_n^3, the Stirling Set of the second kind, denotes the set whose elements cover all the partitions of a set $\{1,2,\cdots,n\}$ into 3 blocks.

In the case $n=3$,

$$H_{3d}\left(\omega_1,\omega_2,\omega_3\right) = c_3^{123}3!a_3M_{111}^{(3)} = 3!a_3c_3^{123}(1)(2)(3)$$

(31)

where

$$c_3^{123} = -\frac{1}{\beta\left(j\omega_1 + j\omega_2 + j\omega_3\right)} \times \frac{1}{3!}$$

(32)

and

$$(1)(2)(3) = \left(j\omega_1\right)H_{1d}\left(\omega_1\right)\left(j\omega_2\right)H_{1d}\left(\omega_2\right)\left(j\omega_3\right)H_{1d}\left(\omega_3\right)$$

(33)

In the case $n=5$,

$$H_{5d}\left(\omega_1,\omega_2,\omega_3,\omega_4,\omega_5\right) = 3!a_3c_5^{12345}M_{113}^{(3)},$$

(34)

where

$$c_5^{12345} = -\frac{1}{\beta\left(\sum_{i=1}^{5}j\omega_i\right)} \times \frac{1}{5!}$$

(35)

$$M_{113}^{(3)} = (5)(4)(321) + (5)(3)(421) + (5)(2)(341) + (5)(1)(324) + (4)(3)(521)$$

+

$$(4)(2)(351) + (4)(1)(325) + (3)(2)(541) + (3)(1)(524) + (2)(1)(354)$$

(36)

where

$$(5)(4)(321) = (j\omega_5)H_{1d}(\omega_5)(j\omega_4)H_{1d}(\omega_4)3!(j\omega_3 + j\omega_2 + j\omega_1)H_{3d}(\omega_3,\omega_2,\omega_1),$$

(37)

and so on.

In the case $n = 7$,

$$H_{7d}(\omega_1,\omega_2,\omega_3,\omega_4,\omega_5,\omega_6,\omega_7) = 3!a_3c_7^{1\cdots7}\left(M_{115}^{(3)} + M_{331}^{(3)}\right)$$

(38)

where

$$c_7^{1\cdots7} = -\frac{1}{\beta\left(\sum_{i=1}^{7} j\omega_i\right)} \times \frac{1}{7!},$$

(39)

$M_{115}^{(3)}$ has 21 terms and is given as

$$\begin{aligned} & M_{115}^{(3)} \\ &= (7)(6)(54321) + (7)(5)(64321) + (7)(4)(56321) + (7)(3)(54621) + (7)(2)(54361) + \\ & (7)(1)(54326) + (6)(5)(74321) + (6)(4)(57321) + (6)(3)(54721) + (6)(2)(54371) + \\ & (6)(1)(54327) + (5)(4)(76321) + (5)(3)(74621) + (5)(2)(74361) + (5)(1)(74326) + \\ & (4)(3)(57621) + (4)(2)(57361) + (4)(1)(57326) + (3)(2)(54761) + (3)(1)(54726) + \\ & (2)(1)(54376) \end{aligned}$$

(40)

$M_{331}^{(3)}$ has 70 terms and is given as

$$\begin{aligned} & M_{331}^{(3)} \\ &= (764)(531)(2) + (764)(521)(3) + (764)(321)(5) + (763)(452)(1) + (763)(451)(2) + \\ & (763)(421)(5) + (763)(521)(4) + (762)(435)(1) + (762)(431)(5) + (762)(451)(3) + \\ & (762)(351)(4) + (761)(432)(5) + (761)(435)(2) + (761)(425)(3) + (761)(325)(4) + \\ & (754)(632)(1) + (754)(631)(2) + (754)(621)(3) + (754)(321)(6) + (753)(462)(1) + \\ & (753)(461)(2) + (753)(421)(6) + (753)(621)(4) + (752)(436)(1) + (752)(431)(6) + \\ & (752)(461)(3) + (752)(361)(4) + (751)(432)(6) + (751)(436)(2) + (751)(426)(3) + \\ & (751)(326)(4) + (743)(652)(1) + (743)(651)(2) + (743)(621)(5) + (743)(521)(6) + \\ & (742)(635)(1) + (742)(631)(5) + (742)(651)(3) + (742)(351)(6) + (741)(632)(5) + \\ & (741)(635)(2) + (741)(625)(3) + (741)(325)(6) + (732)(465)(1) + (732)(461)(5) + \\ & (732)(451)(6) + (732)(651)(4) + (731)(462)(5) + (731)(465)(2) + (731)(425)(6) + \\ & (731)(625)(4) + (721)(436)(5) + (721)(435)(6) + (721)(465)(3) + (721)(365)(4) + \\ & (654)(321)(7) + (653)(421)(7) + (652)(431)(7) + (651)(432)(7) + (643)(521)(7) + \\ & (642)(351)(7) + (641)(325)(7) + (632)(451)(7) + (631)(425)(7) + (621)(435)(7) \end{aligned}$$

(41)

where

$$\begin{aligned} & (7)(6)(54321) \\ &= (j\omega_7)H_1(\omega_7)(j\omega_6)H_1(\omega_6)5!(j\omega_5 + j\omega_4 + j\omega_3 + j\omega_2 + j\omega_1)H_5(\omega_5,\omega_4,\omega_3,\omega_2,\omega_1) \end{aligned}$$

(42)

$$\begin{aligned} & (764)(531)(2) \\ &= 3!(j\omega_7 + j\omega_6 + j\omega_4)H_3(\omega_7,\omega_6,\omega_4)3!(j\omega_5 + j\omega_3 + j\omega_1)H_3(\omega_5,\omega_3,\omega_1)(j\omega_2)H_1(\omega_2) \end{aligned}$$

(43)

and so on.

In the case $n = 9$,

$$H_{9d}\left(\omega_1,\omega_2,\omega_3,\omega_4,\omega_5,\omega_6,\omega_7,\omega_8,\omega_9\right) = 3!a_3c_9^{1\cdots9}\left(M_{117}^{(3)} + M_{135}^{(3)} + M_{333}^{(3)}\right)$$

(44)

where

$$c_9^{1\cdots9} = -\frac{1}{\beta\left(\sum_{i=1}^{9} j\omega_i\right)} \times \frac{1}{9!}$$

(45)

$M_{117}^{(3)}$, $M_{135}^{(3)}$ and $M_{333}^{(3)}$ have 36, 504 and 280 terms respectively. These expressions are omitted here due to space limitations, but the results will be used in section 6 to obtain a more accurate analysis of the system output frequency response.

More GFRFs for $y_d\left(t\right)$ can be derived easily according to Eqs. (26) – (30).

4.2.2 Derivation of the GFRFs for $y_F\left(t\right)$

Substituting Eq. (8) into Eq. (7) yields

$$m\ddot{y}_d\left(t\right) + y_F\left(t\right) = u\left(t\right)$$

(46)

According to Eq. (23), the second-order derivative of $y_d\left(t\right)$ can be expressed as

$$\ddot{y}_d\left(t\right) = n!\left(j\sum_{i=1}^{n}\omega_i\right)^2 H_{nd}\left(j\omega_1,\cdots,j\omega_n\right)e^{jt\sum_{i=1}^{n}\omega_i} + etc.$$

(47)

$y_F\left(t\right)$ can be written as

$$y_F\left(t\right) = n!\,H_{nF}\left(j\omega_1,\cdots,j\omega_n\right)e^{jt\sum_{i=1}^{n}\omega_i} + etc.$$

(48)

Substituting Eqs. (47), (48) and (16) into Eq. (46) gives

$$m\cdot n!\left(j\sum_{i=1}^{n}\omega_i\right)^2 H_{nd}\left(j\omega_1,\cdots,j\omega_n\right)e^{jt\sum_{i=1}^{n}\omega_i} + n!\,H_{nF}\left(j\omega_1,\cdots,j\omega_n\right)e^{jt\sum_{i=1}^{n}\omega_i} + etc. = \sum_{i=1}^{R}e^{j\omega_i t}$$

(49)

When $n = 1$, equating the coefficients of $e^{j\omega_1 t}$ from Eq. (49) yields

$$m\left(j\omega_1\right)^2 H_{1d}\left(j\omega_1\right) + H_{1F}\left(j\omega_1\right) = 1$$

(50)

Therefore,

$$H_{1F}\left(j\omega_1\right)=1-m\left(j\omega_1\right)^2 H_{1d}\left(j\omega_1\right)$$

(51)

Substituting Eq. (25) into Eq. (51) gives

$$H_{1F}\left(\omega_1\right)=\frac{a_1\left(j\omega_1\right)+k}{\beta\left(j\omega_1\right)}$$

(52)

When $n\geq 2$, equating the coefficients of $e^{jt\sum_{i=1}^{n}\omega_i}$ from Eq. (49) yields

$$m\cdot n!\left(j\sum_{i=1}^{n}\omega_i\right)^2 H_{nd}\left(j\omega_1,\cdots,j\omega_n\right)+n!H_{nF}\left(j\omega_1,\cdots,j\omega_n\right)=0$$

(53)

That is

$$H_{nF}\left(j\omega_1,\cdots,j\omega_n\right)=-m\left(j\sum_{i=1}^{n}\omega_i\right)^2 H_{nd}\left(j\omega_1,\cdots,j\omega_n\right)$$

(54)

The GFRFs for $y_F\left(t\right)$ ($n\geq 2$) can be given by substituting the expressions of $H_{nd}\left(j\omega_1,\cdots,j\omega_n\right)$ derived in Section 4.2.1 into Eq. (54).

4.3. The effects of system nonlinearity on the output frequency response

The expressions for the system GFRFs in terms of the nonlinear damping characteristic parameters can now be used to derive an expression for the output spectrum $Y_F\left(j\omega\right)$. Substituting the expressions for higher order GFRFs derived in section 4.2 into Eq. (15) yields

$$\begin{aligned}Y_F\left(j\omega\right)&=\sum_{n=1}^{N}\frac{1}{2^n}\sum_{\omega_{k_1}+\cdots+\omega_{k_n}=\omega}H_{nF}\left(j\omega_{k_1},\cdots,j\omega_{k_n}\right)A\left(\omega_{k_1}\right)\cdots A\left(\omega_{k_n}\right)\\&=\frac{1}{2}H_{1F}\left(j\omega\right)A\left(\omega\right)+\frac{1}{2^3}\sum_{\omega_{k_1}+\omega_{k_2}+\omega_{k_3}=\omega}\left[H_{3F}\left(j\omega_{k_1},j\omega_{k_2},j\omega_{k_3}\right)\prod_{i=1}^{3}A\left(\omega_{k_i}\right)\right]+\cdots\\&=\frac{1}{2}H_{1F}\left(j\omega\right)A\left(\omega\right)+\frac{1}{2^3}\sum_{\omega_{k_1}+\omega_{k_2}+\omega_{k_3}=\omega}\left[-m\left(j\sum_{i=1}^{3}\omega_{k_i}\right)^2 3!a_3c_3^{123}(1)(2)(3)\prod_{i=1}^{3}A\left(\omega_{k_i}\right)\right]+\cdots\\&=p_1\left(j\omega\right)+p_3\left(j\omega\right)a_3+\cdots\end{aligned}$$

(55)

where

$$p_1\left(j\omega\right)=\frac{1}{2}H_{1F}\left(j\omega\right)A\left(\omega\right)$$

(56)

$$p_3(j\omega)=\frac{1}{2^3}\sum_{\omega_{k_1}+\omega_{k_2}+\omega_{k_3}=\omega}\left[-m\left(j\sum_{i=1}^{3}\omega_{k_i}\right)^2 3!c_3^{123}(1)(2)(3)\prod_{i=1}^{3}A\left(\omega_{k_i}\right)\right]$$

(57)

Generally,

$$Y_F(j\omega)=\sum_{k=0}^{\lfloor (N-1)/2\rfloor}\left(p_{2k+1}a_3^{\,k}\right)$$

(58)

where $\left\lfloor\frac{N-1}{2}\right\rfloor$ denotes the floor function, also called the greatest integer function or integer value, which gives the largest integer less than or equal to $\frac{N-1}{2}$.

Note that $p_i(j\omega)$, $i=1,3,\cdots$, produced by the system GFRFs, depends on the applied multi-tone input and the parameters which describe the linear characteristic of the system but are independent of a_3.

Denote

$$P_{2k+1}=p_{2k+1}a_3^{\,k}$$

(59)

Then substituting Eq. (59) into Eq. (58) gives

$$Y_F(j\omega)=\sum_{k=0}^{\lfloor (N-1)/2\rfloor}P_{2k+1}$$

(60)

Eq. (60) is a very important result which describes the relationship between the system frequency response and the characteristic parameters of the system nonlinearity. The result extends the fundamental analytical relationship between the linear characteristic parameters and the output frequency response to the nonlinear case for system (2) and (3) when the system is subject to a multi-tone input, and can be easily extended to other general situations.

For a given multi-tone input and the linear characteristic parameters m, a_1, k, $p_i(j\omega)$, $i=1,2,\cdots$ in Eq. (60) are known functions of frequency ω. Eq. (60) indicates that at each frequency component the system output spectrum is a polynomial function of the nonlinear damping characteristic parameter a_3.

When the system is subject to the harmonic input (6), and the output frequency of interest in the analysis is the same as the input frequency Ω,

$$Y_F(j\Omega)=\sum_{n=1}^{N}\frac{1}{2^n}\sum_{\omega_{k_1}+\cdots+\omega_{k_n}=\Omega}H_{nF}\left(j\omega_{k_1},\cdots,j\omega_{k_n}\right)A\left(\omega_{k_1}\right)\cdots A\left(\omega_{k_n}\right)$$

$$= \frac{1}{2} H_{1F}\left(j\Omega \right) A\left(\Omega \right) + \frac{1}{2^3} \sum_{\omega_{k_1}+\omega_{k_2}+\omega_{k_3}=\Omega} \left[H_{3F}\left(j\omega_{k_1}, j\omega_{k_2}, j\omega_{k_3} \right) \prod_{i=1}^{3} A\left(\omega_{k_i} \right) \right] + \cdots$$

(61)

where

$$\sum_{\omega_{k_1}+\omega_{k_2}+\omega_{k_3}=\Omega} \left[H_{3F}\left(j\omega_{k_1}, j\omega_{k_2}, j\omega_{k_3} \right) \prod_{i=1}^{3} A\left(\omega_{k_i} \right) \right]$$

$$= H_{3F}\left(-\Omega, \Omega, \Omega \right) A\left(-\Omega \right) A\left(\Omega \right) A\left(\Omega \right) + H_{3F}\left(\Omega, -\Omega, \Omega \right) A\left(\Omega \right) A\left(-\Omega \right) A\left(\Omega \right)$$

$$+ H_{3F}\left(\Omega, \Omega, -\Omega \right) A\left(\Omega \right) A\left(\Omega \right) A\left(-\Omega \right)$$

$$= \left| A\left(\Omega \right) \right|^2 A\left(\Omega \right) \left[H_{3F}\left(-\Omega, \Omega, \Omega \right) + H_{3F}\left(\Omega, -\Omega, \Omega \right) + H_{3F}\left(\Omega, \Omega, -\Omega \right) \right]$$

(62)

Since GFRF $H_n\left(j\omega_1, \cdots, j\omega_n \right)$ is symmetric,

$$H_{3F}\left(-\Omega, \Omega, \Omega \right) = H_{3F}\left(\Omega, -\Omega, \Omega \right) = H_{3F}\left(\Omega, \Omega, -\Omega \right)$$

(63)

Substituting Eq. (63) into Eq. (62) yields

$$\sum_{\omega_{k_1}+\omega_{k_2}+\omega_{k_3}=\Omega} \left[H_{3F}\left(j\omega_{k_1}, j\omega_{k_2}, j\omega_{k_3} \right) \prod_{i=1}^{3} A\left(\omega_{k_i} \right) \right] = 3H_{3F}\left(-\Omega, \Omega, \Omega \right) \left| A\left(\Omega \right) \right|^2 A\left(\Omega \right)$$

(64)

Generally,

$$\sum_{\omega_{k_1}+\cdots+\omega_{k_n}=\Omega} H_{nF}\left(j\omega_{k_1}, \cdots, j\omega_{k_n} \right) A\left(\omega_{k_1} \right) \cdots A\left(\omega_{k_n} \right) = C\left(n, \left\lfloor \frac{n}{2} \right\rfloor \right) H_{n, \left\lfloor \frac{n}{2} \right\rfloor} \left| A\left(\Omega \right) \right|^{\left\lfloor \frac{n}{2} \right\rfloor} A\left(\Omega \right)$$

(65)

where $H_{n, \left\lfloor \frac{n}{2} \right\rfloor}\left(\Omega, \cdots, \Omega, -\Omega, \cdots, -\Omega \right)$ is a higher-order GFRF with $n - \left\lfloor \frac{n}{2} \right\rfloor$ arguments of Ω and $\left\lfloor \frac{n}{2} \right\rfloor$ arguments of $-\Omega$ and $C\left(n, \left\lfloor \frac{n}{2} \right\rfloor \right)$ is the number of combinations of $\left\lfloor \frac{n}{2} \right\rfloor$ objects from a set with n objects and given as

$$C\left(n, \left\lfloor \frac{n}{2} \right\rfloor \right) = \frac{n!}{\left\lfloor \frac{n}{2} \right\rfloor ! \left(n - \left\lfloor \frac{n}{2} \right\rfloor \right)!}$$

(66)

Substituting Eq. (65) into Eq. (61) gives

$$Y_F\left(j\Omega \right) = \sum_{n=1}^{N} \frac{1}{2^n} C\left(n, \left\lfloor \frac{n}{2} \right\rfloor \right) \left| A\left(\Omega \right) \right|^{\left\lfloor \frac{n}{2} \right\rfloor} A\left(\Omega \right) H_{n, \left\lfloor \frac{n}{2} \right\rfloor}$$

(67)

Eq. (67) can also be written as

$$Y_F(j\Omega) = \sum_{n=1}^{N} P_n$$

(68)

where

$$P_n = \frac{1}{2^n} C\left(n, \left\lfloor \frac{n}{2} \right\rfloor\right) \left|A(\Omega)\right|^{\left\lfloor \frac{n}{2} \right\rfloor} A(\Omega) H_{n, \frac{n}{2}}$$

(69)

Eq. (68) shows that the output energy at the driving frequency Ω contributed by the linear term $\frac{1}{2}A(\Omega)H_{1,0}$ is modified by the higher-order system nonlinear effects to yield the output frequency response $Y_F(j\Omega)$.

Simulation studies will be conducted in section 5 for systems (2) and (3) to evaluate the output frequency response to the harmonic input (6) for different damping characteristics. The results will then be compared with the output spectrum $Y_F(j\Omega)$ determined using Eq. (68) in section 6. The objective is to investigate how a nonlinearity reduces the energy in the output spectrum at the driving frequency and modifies the energy distribution and to present a new approach to suppress resonant vibration by designing the system nonlinearity.

5. Simulation Studies

Consider the system (2) and (3) subject to the harmonic input (6). Take the system linear characteristic and input parameters as follows:

m=240 kg, k=16000 N m^{-1}, a_1=29.6 s N m^{-1}, F_d=100 N, Ω=8.1 rad s^{-1}

where Ω=8.1 rad s^{-1} corresponds to the natural undamped frequency. The damping characteristic is defined by $f(\bullet) = a_1(\bullet) + a_3(\bullet)^3$.

5.1 Systems Stability

Define the state of the system as follows

$$\begin{cases} x_1 = x \\ x_2 = \dot{x} \end{cases}$$

(70)

The state space equation of system (7) without the disturbance input $u(t) = F_d \cos(\Omega t)$ can be expressed as

$$\begin{cases} \dot{x}_1 = x_2 \\ \dot{x}_2 = -\frac{1}{m}\left(a_1 x_2 + a_3 x_2^{\,3} + k x_1\right) \end{cases}$$

(71)

Choose a Lyapunov function as

$$V(x,t) = \frac{1}{2}kx_1^2 + \frac{1}{2}mx_2^2$$

(72)

Taking the derivative of V along trajectories of the system gives

$$\begin{aligned}\dot{V} &= \begin{bmatrix} kx_1 & mx_2 \end{bmatrix} \begin{bmatrix} \dot{x}_1 \\ \dot{x}_2 \end{bmatrix} \\ &= \begin{bmatrix} kx_1 & mx_2 \end{bmatrix} \begin{bmatrix} x_2 \\ -\frac{1}{m}\left(a_1 x_2 + a_3 x_2^3 + kx_1\right) \end{bmatrix} \\ &= -\left(a_1 x_2^2 + a_3 x_2^4\right)\end{aligned}$$

(73)

The function $\dot{V}$ can be made negative definite if $\begin{cases} a_1 > 0 \\ a_3 > 0 \end{cases}$, and hence the system is asymptotically stable at $x_1 = x_2 = 0$. Additionally, if $\begin{cases} a_1 > 0 \\ a_3 > 0 \end{cases}$, the system with a disturbance input is asymptotically stable to a ball [16].

5.2 Simulation Studies

Since the system is always stable if $\begin{cases} a_1 > 0 \\ a_3 > 0 \end{cases}$ according to section 5.1, the value of the nonlinear damping parameter a_3 can be any positive real number. The system was simulated to generate the output frequency response $Y_F(j\Omega)$ for the following three cases:

(i) $f(\bullet) = a_1(\bullet) + a_3(\bullet)^3$ where $a_3 = 0$ s N m^{-1}

(ii) $f(\bullet) = a_1(\bullet) + a_3(\bullet)^3$ where $a_3 = 1\times10^3$ s N m^{-1}

(iii) $f(\bullet) = a_1(\bullet) + a_3(\bullet)^3$ where $a_3 = 1\times10^6$ s N m^{-1}

Figs. 2, 3 and 4 show the numerical simulation results of the output spectrum obtained by performing a FFT operation on the system time domain output $y_F(t)$ for cases (i), (ii) and (iii) respectively.

The numerical simulation results indicate that the magnitude of the system output spectrum $2\left|Y_F(j\Omega)\right|$ at $\Omega = 8.1$ rad s^{-1} reduces from 4585.0818 N to 959.0752 N as the nonlinear damping characteristic parameter a_3 increases from 0 sN/m where the system is linear to 1×10^3 s N m^{-1}. Then when a_3 increases to 1×10^6 s N m^{-1}, $2\left|Y_F(j\Omega)\right|$ reduces again to 136.4987 s N m^{-1}. Figs. 2, 3 and 4 also clearly show that some of the energy at the excitation frequency $\Omega = 8.1$ rad s^{-1} is transferred to higher frequencies. Therefore, nonlinear damping can reduce the output energy at the driving frequency and at the same time spread the output signal energy over a wider range of harmonics. This reduction at the resonance becomes larger as the

nonlinearity gets stronger.

5.3 Other damping characteristic cases

In order to investigate the way in which nonlinearity modifies the energy distribution, three other damping characteristic cases are studied in this section:

(iv) $f(\bullet) = a_1(\bullet) + a_3(\bullet)^3 + a_5(\bullet)^5$ where $a_3 = 1\times10^3$ s N m^{-1} and $a_5 = 1\times10^6$ s N m^{-1}

(v) $f(\bullet) = a_1(\bullet) + a_2|(\bullet)| + a_3(\bullet)^3$ where $a_2 = 20$ s N m^{-1} and $a_3 = 1\times10^3$ s N m^{-1}

(vi) $f(\bullet) = a_1(\bullet) + a_2\left(10^{(\bullet)} - 1\right)$ where $a_2 = 1\times10^3$ s N m^{-1}

The numerical simulation results of the output spectrum for cases (iv), (v) and (vi) are shown by Figs. 5, 6 and 7 respectively.

5.4 Simulation conclusions

5.4.1 Proposition 1

The magnitude reduction percentage and the relative nonlinearity will be defined below and used to assess the simulation results.

The Magnitude Reduction Percentage (MRP) is defined as

$$[MRP] = \frac{2\left|Y_F{}^L\left(j\Omega_i\right)\right| - 2\left|Y_F{}^{NL}\left(j\Omega_i\right)\right|}{2\left|Y_F{}^L\left(j\Omega\right)\right|}\times100\%$$

(74)

where $2\left|Y_F{}^L\left(j\Omega_i\right)\right|$ is the magnitude of $Y_F\left(j\Omega\right)$ at the dominant frequency when $f(\cdot)$ is a linear function and $2\left|Y_F{}^{NL}\left(j\Omega_i\right)\right|$ is the magnitude of $Y_F\left(j\Omega\right)$ at the dominant frequency when $f(\cdot)$ is a nonlinear function.

The Relative Nonlinearity (RN) is defined as

$$[RN] = \frac{df(\cdot)/d(\cdot)}{a_1}$$

(75)

From the simulation results and the definitions above, a summary of the results relating to the six cases are given in Table 1.

Proposition 1 easily follows by inspection of Figs. 2-7 and Table 1.

Proposition 1: When the input magnitude F_d and the input frequency Ω are fixed, $[MRP]$ will increase if $[RN]$ increases.

5.4.2 Proposition 2

Proposition 2: In most cases, there will be much less power at the harmonics in the

output spectrum when $f(\cdot)$ is an odd function than when it is not.

Proposition 2 easily follows by comparing the Bode response in Figs. 2-5 to Fig. 6.

The proof is given as follows.

Proof:

Let $$f(\cdot)=\sum_{k=1}^{N} a_{2k-1}(\cdot)^{2k-1}$$

(76)

The equilibrium equation for the system in Fig. 1 and corresponding force at the support can be expressed as

$$m\ddot{y}_d(t)+\sum_{k=1}^{N} a_{2k-1}\dot{y}_d{}^{2k-1}(t)+ky_d(t)=u(t)$$

(77)

$$y_F(t)=\sum_{k=1}^{N} a_{2k-1}\dot{y}_d{}^{2k-1}(t)+ky_d(t)$$

(78)

Since $a_{2k}=0$ where $k=1,2,3,\cdots$ in Eq. (77),

$$H_{2kd}(j\omega_1,\cdots,j\omega_n)=0$$

(79)
[17].

Following the procedure of section 4.2.2 yields

$$H_{nF}(j\omega_1,\cdots,j\omega_n)=-m\left(j\sum_{i=1}^{n}\omega_i\right)^2 H_{nd}(j\omega_1,\cdots,j\omega_n)$$

(80)

Substituting Eq. (79) into Eq. (80) gives

$$H_{2kF}(j\omega_1,\cdots,j\omega_n)=0\,,\quad k=1,2,3,\cdots$$

(81)

Substituting Eq. (81) into Eq. (55) yields

$$Y_F(j\omega)=\sum_{i=0}^{N}\frac{1}{2^{2i-1}}\sum_{\omega_{k_1}+\omega_{k_2}\cdots+\omega_{k_{2i-1}}=\omega} H_{(2i-1)F}(j\omega_{k_1},j\omega_{k_2},\cdots,j\omega_{k_{2i-1}})A(\omega_{k_1})A(\omega_{k_2})\cdots A(\omega_{k_{2i-1}})$$

(82)

When the system is subject to the harmonic input (6),

$$\omega_{k_{2i-1}}=\pm\Omega\,,\quad i=1,2,3,\cdots$$

(83)

Therefore,

$$\omega = \omega_{k_1} + \omega_{k_2} \cdots + \omega_{k_{2i-1}} = \pm\Omega, \pm 3\Omega, \pm 5\Omega, \cdots$$

(84)

That is

$$Y_F(j2k\Omega) = 0,\ k = 1, 2, 3, \cdots$$

(85)

which means that the energy at the even harmonics is transferred to the odd harmonics and the number of harmonics in the output spectrum when $f(\cdot)$ is an odd function is only half that when it is not odd. This completes the proof.

5.4.3 Summary

According to proposition 1 and 2, a nonlinear damping element described by the odd polynomial function $f(\cdot) = \sum_{l=1}^{N} a_{2l-1}(\cdot)^{2l-1}$ can be introduced between the incoming signal and the structure of interest to suppress resonant vibrations.

6. Analysis

Consider the system (2) and (3) subject to the harmonic input (6) and using the following system linear characteristic and input parameters:

m=240 kg, k=16000 N m^{-1}, a_1=29.6 s N m^{-1}, F_d=10 N, Ω=8.1 rad s^{-1}

where Ω=8.1 rad s^{-1} is corresponding to the natural undamped frequency.

In order to investigate how nonlinearity reduces the energy in the output spectrum at the driving frequency, the output spectra $Y_F(j\Omega)$ are determined using Eq. (68) and the expressions of the GFRFs for $y_F(t)$ derived in section 4.2, and the results obtained are then compared to the results obtained by simulation for three different damping characteristics as follows:

(vii) $f(\bullet) = a_1(\bullet) + a_3(\bullet)^3$ where $a_3 = 0$ s N m^{-1}

(viii) $f(\bullet) = a_1(\bullet) + a_3(\bullet)^3$ where $a_3 = 100$ s N m^{-1}

(ix) $f(\bullet) = a_1(\bullet) + a_3(\bullet)^3$ where $a_3 = 200$ s N m^{-1}

Figs. 8, 9 and 10 show the results for cases (vii), (viii) and (ix) respectively. In Figs. 8, 9 and 10, the solid lines show the output spectrum $Y_F(j\Omega)$ at the driving frequency determined using the analytical description (68) when the system nonlinearities up to ninth order are taken into account. The dashed lines show the numerical simulation results of the output spectrum obtained by performing a FFT operation on the system time domain output $y_F(t)$.

Inspection of Figs. 8, 9 and 10 clearly shows that the output energy at the driving frequency Ω contributed by the linear term $P1$ is modified by the higher-order system nonlinear effects P_n $(n \geq 2)$ to yield the output frequency response $Y_F(j\Omega)$.

Comparing Figs. 9 and 10 indicates that the cancellation between the linear term and the higher-order system nonlinear effects becomes larger when the nonlinearity becomes stronger.

The general case when the nonlinear damping characteristic is described by a polynomial function can be analyzed using the same set of procedures. In mathematics, the Weierstrass Approximation Theorem [18] guarantees that any continuous function on a closed and bounded interval can be uniformly approximated on that interval by a polynomial to any degree of accuracy. Therefore, other nonlinear damping characteristics which are not directly described by a polynomial can be approximated by a polynomial function and then analyzed by this method.

7. Conclusions

The relationship between the output frequency response and the nonlinear damping characteristic parameters of an sdof spring damper system has been studied. The studies demonstrate that the nonlinear damping element can reduce the output energy at the driving frequency and at the same time spread the output signal energy over a wide range of harmonics. It has also been shown that the reduction becomes larger as the nonlinear damping characteristic gets stronger and in most cases, there will be much less power at the harmonics in the output spectrum if the nonlinear damping characteristic is an odd function. Hence, an odd polynomial nonlinear damping element can be introduced between the incoming signal and the structure of interest to move the energy into higher harmonic frequencies with a corresponding reduction in the level of the output at the driving frequency. The transmitted force spectrum was also expressed in terms of the nonlinear generalized frequency response functions to show how the energy, at the excitation frequency, is modified by the nonlinearity.

Acknowledgement

B.Z. acknowledges the support provided by Sheffield University under the scholarship scheme and the Overseas Research Student (ORS) Award of UK. S.A.B., Z.Q.L. and G.R.T. gratefully acknowledge that part of this work was supported by EPSRC of UK.

References

[1] A. Maccari, Vibration control for thr primary resonance of a cantilever beam by a time delay state feedback. *Journal of Sound and Vibration* 259 (2003) 241-251.

[2] H. K. Jang, Design guideline for the improvement of dynamic comfort of a vehicle seat and its application. International *Journal of Automotive Technology* 6 (2005) 383-390.

[3] S. Yang, S. P. Choi and Y. C. Kim, Vibratin reduction optimum design of a steam-turbine rotor-bearing system using a hybrid genetic algorithm. *Structure and Multidisciplinary Optimization* 30 (2005) 43-53.

[4] P. Museros and E. Alarcon, Influence of the second bending mode on the response of high-speed bridges at resonance. *Journal of Structural Engineering* 131 (2005) 405-415.

[5] S. S. Oueni, A. H. Nayfeh and J. R. Pratt, A nonlinear vibration absorber for flexible structures. *Nonlinear Dynamics* 15 (1998) 259-282.
[6] N. Jalili and D. W. Knowles, Structural vibration control using an active resonator absorber: modelling and control implementation. *Smart Materials & Structures* 13 (2004) 998-1005.
[7] V. Volterra, *Theory of Functionals and of Integral and Integro-differential Equations*, Dover Publications, New York, 1959.
[8] M. Schetzen, *The Volterra and Wiener Theories of Nonlinear Systems*, Wiley Interscience Publications, New York, 1980.
[9] Z.Q. Lang, S.A. Billings, Output frequency characteristics of nonlinear systems. *International Journal of Control* 64 (1996) 1049–1067.
[10] A.K. Swain, S.A. Billings, Generalised frequency response function matrix for MIMO nonlinear systems. *International Journal of Control* 74 (2001) 829–844.
[11] K. Worden, G. Manson, G.R. Tomlinson, A harmonic probing algorithm for the multi-input Volterra series. *Journal of Sound and Vibration* 201 (1997) 67–84.
[12] E. Bedrosian, S.O. Rice, The output properties of Volterra systems (nonlinear systems with memory) driven by harmonic and Gaussian input. *Proceedings of the IEEE* 59 (1971) 1688–1707.
[13] J.J Bussgang, L. Ehrman and J.W. Graham, 1974, Analysis of nonlinear systems with multiple inputs. *Proceedings of the IEEE* 62 (1974) 1088-1119.
[14] W.J. Rugh, *Nonlinear System theory—The Volterra/Wiener Approach*, Johns Hopkins University Press, Baltimore and London, 1981.
[15] Zhang, S.A. Billings, Z.Q. Lang and G.R. Tomlinson, *Analytical description of the frequency response function of the generalized Duffing oscillator model*, Research report 945, Department of Automatical Control & Systems Engineering, Sheffield University, 2006.
[16] X.J. Jing, Z.Q. Lang and S.A. Billings, Frequency domain analysis based nonlinear feedback control for suppressing periodic disturbance. *Proceedings of the 6th World Congress on Intelligent Control and Automation*, Dalian, China, June 2006, 1161–1165.
[17] X.J. Jing, Z.Q. Lang, S.A. Billings and G.R. Tomlinson, The parametric characteristic of frequency response functions for nonlinear systems. *International Journal of Control* 79 (2006) 1552 - 1564.
[18] H. Jeffreys and B. S. Jeffreys, *Methods of Mathematical Physics*, Cambridge University Press, 1988.

Table 1
Simulation results of cases (i)-(vi)

Case number	$f(\dot{x})$ ($a_1 = 29.6$ s N m^{-1})		$2\left\|Y_F^{NL}(j\Omega_i)\right\|$ (N)	$[MRP]$
i	$f(\bullet) = a_1(\bullet)$		*4.5851e+003*	0%
ii	$f(\bullet) = a_1(\bullet) + a_3(\bullet)^3$ $\dot{x} \in [-0.5, 0.5]$	$a_3 = 1\times10^3$ s N m^{-1}	959.0752	79.0828%
iii	$f(\bullet) = a_1(\bullet) + a_3(\bullet)^3$ $\dot{x} \in [-0.05, 0.05]$	$a_3 = 1\times10^6$ s N m^{-1}	136.4987	97.0230%

iv	$f(\bullet) = a_1(\bullet) + a_3(\bullet)^3 + a_5(\bullet)^5$ $\dot{x} \in [-0.2, 0.2]$	$a_3 = 1\times10^3$ s N m^{-1}, $a_5 = 1\times10^6$ s N m^{-1}	346.9872	92.4323%
v	$f(\bullet) = a_1(\bullet) + a_2\lvert(\bullet)\rvert + a_3(\bullet)^3$ $\dot{x} \in [-0.5, 0.5]$	$a_3 = 1\times10^3$ s N m^{-1}, $a_2 = 20$ s N m^{-1}	959.0655	79.0830%
vi	$f(\bullet) = a_1(\bullet) + a_2\left(10^{(\bullet)} - 1\right)$ $\dot{x} \in [-0.045, 0.045]$	$a_2 = 1\times10^3$ s N m^{-1}	130.9598	97.1438%

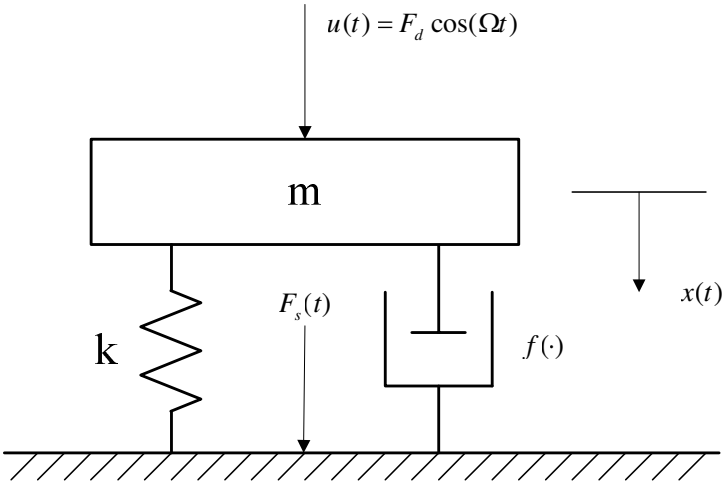

Fig. 1. The SDOF mass-spring-damper system considered in the study

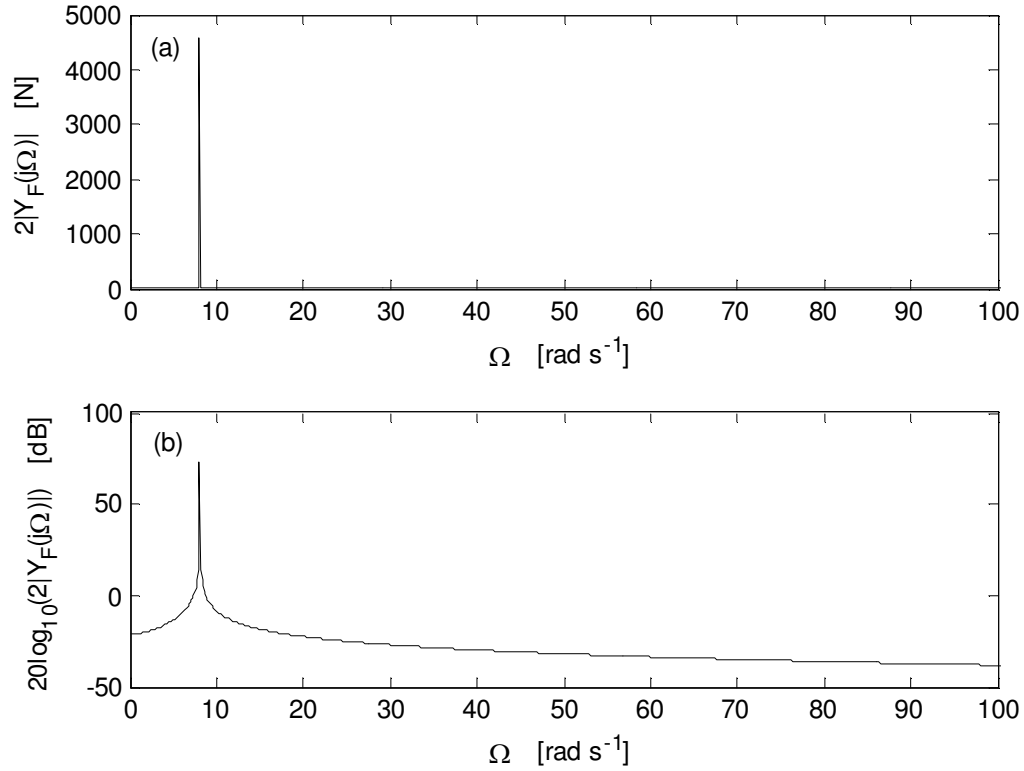

Fig. 2. The output frequency response when $f(\bullet) = a_1(\bullet) + a_3(\bullet)^3$, $a_1 = 29.6$ s N m^{-1} and $a_3 = 0$ s N m^{-1}: (a) Amplitude response, (b) Bode response.

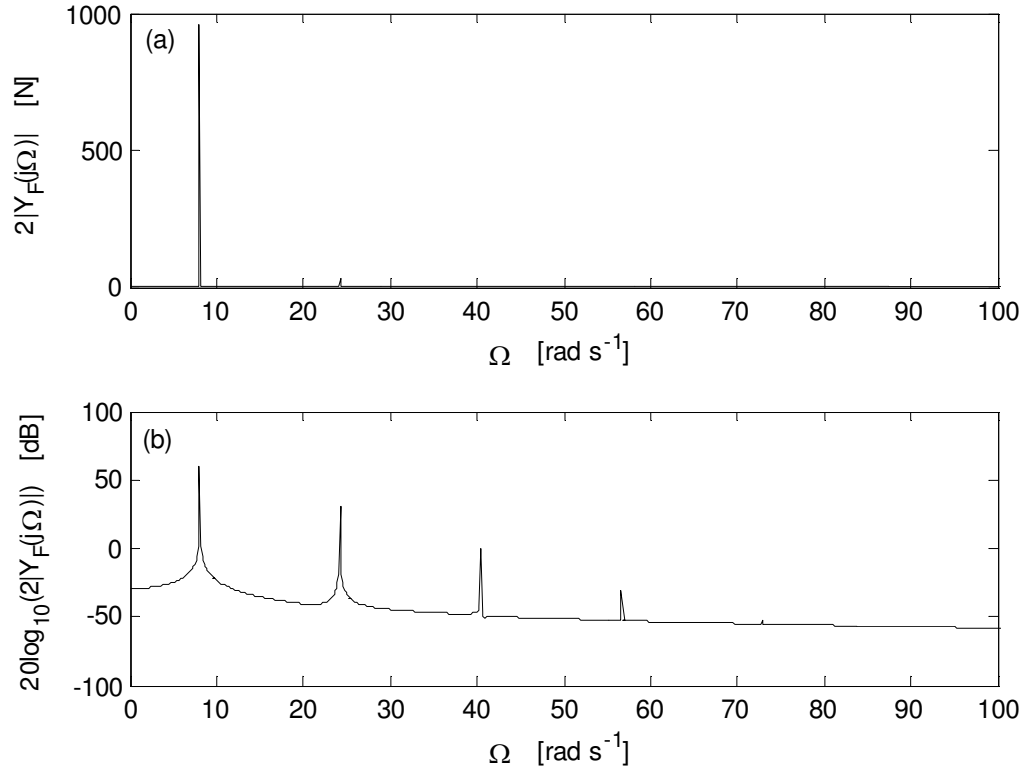

Fig. 3. The output frequency response when $f(\bullet) = a_1(\bullet) + a_3(\bullet)^3$, $a_1 = 29.6$ s N m^{-1} and

$a_3 = 1 \times 10^3$ s N m^{-1}: (a) Amplitude response, (b) Bode response.

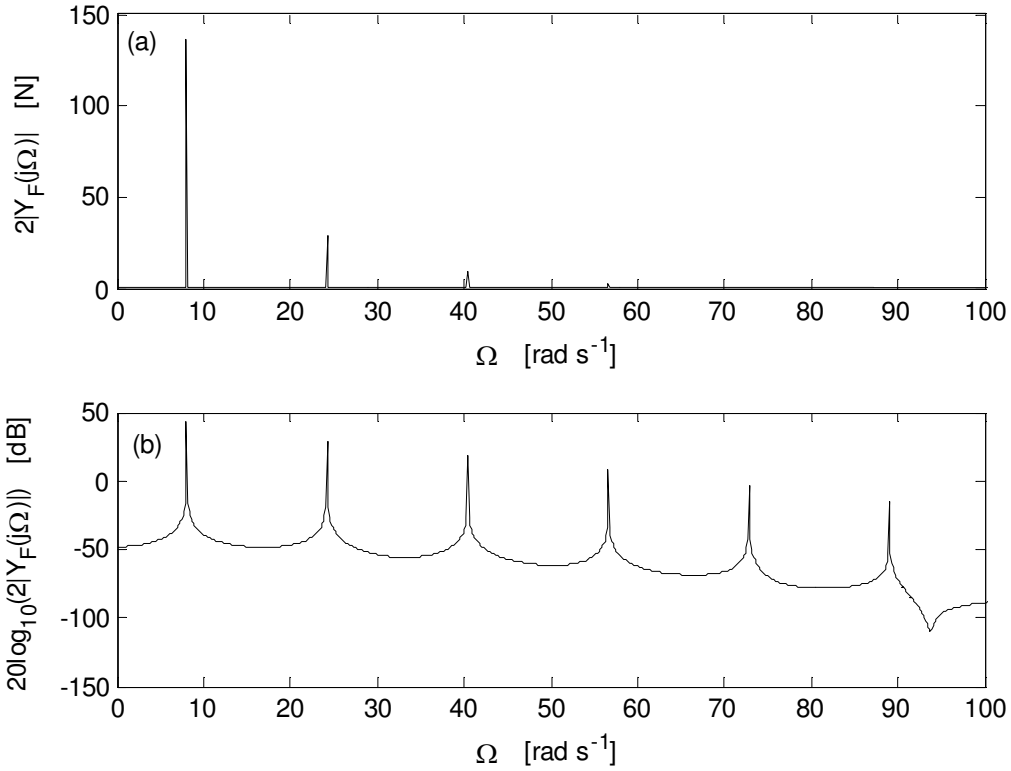

Fig. 4. The output frequency response when $f(\bullet) = a_1(\bullet) + a_3(\bullet)^3$, $a_1 = 29.6$ s N m^{-1} and $a_3 = 1 \times 10^6$ s N m^{-1}: (a) Amplitude response, (b) Bode response.

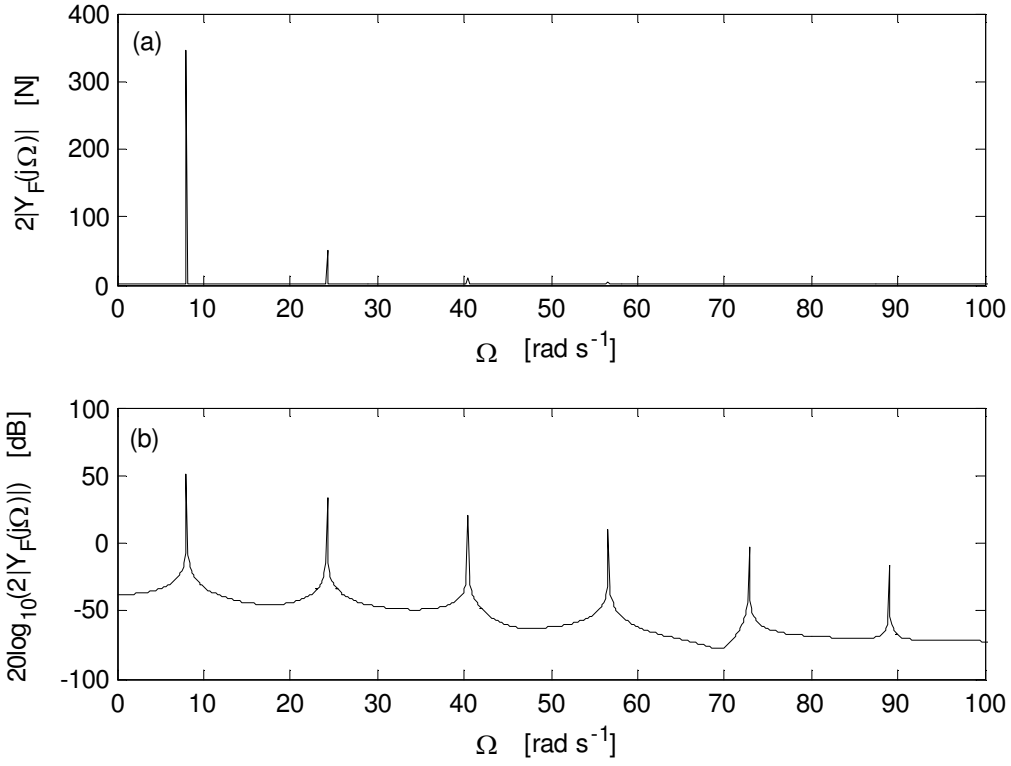

Fig. 5. The output frequency response when $f(\bullet) = a_1(\bullet) + a_3(\bullet)^3 + a_5(\bullet)^5$, $a_1 = 29.6$ s N m^{-1}, $a_3 = 1 \times 10^3$ s N m^{-1} and $a_5 = 1 \times 10^6$ s N m^{-1}: (a) Amplitude response, (b) Bode response.

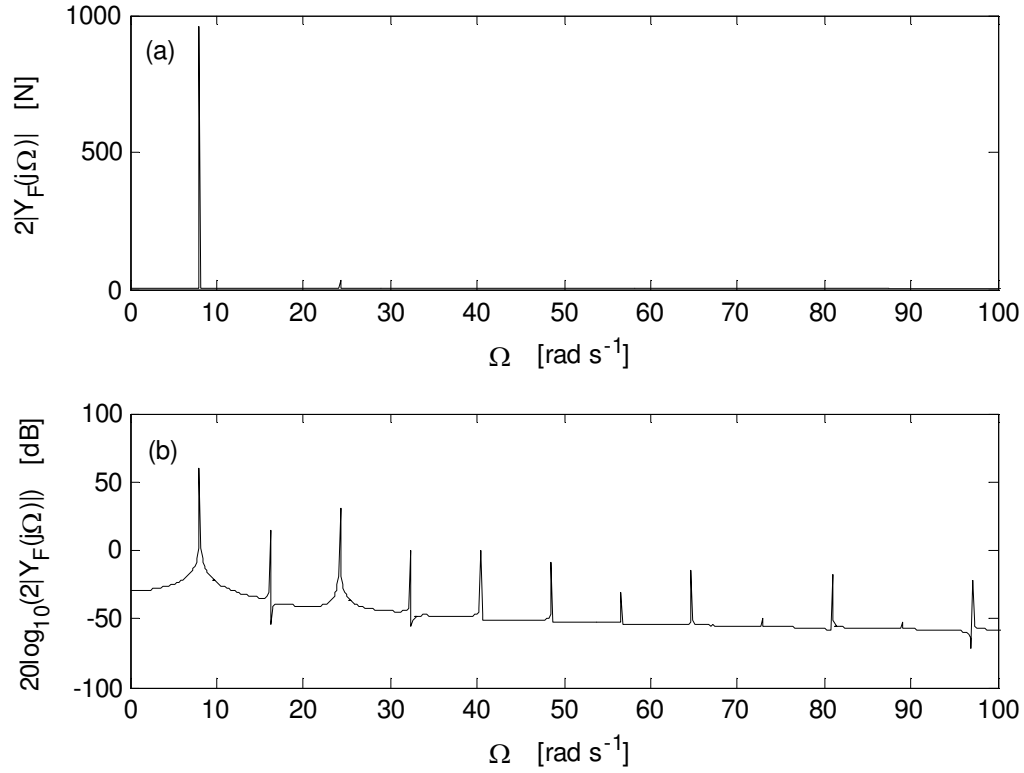

Fig. 6. The output frequency response when $f(\bullet) = a_1(\bullet) + a_2 |(\bullet)| + a_3(\bullet)^3$, $a_1 = 29.6$ s N m^{-1}, $a_2 = 20$ s N m^{-1} and $a_3 = 1 \times 10^3$ s N m^{-1}: (a) Amplitude response, (b) Bode response.

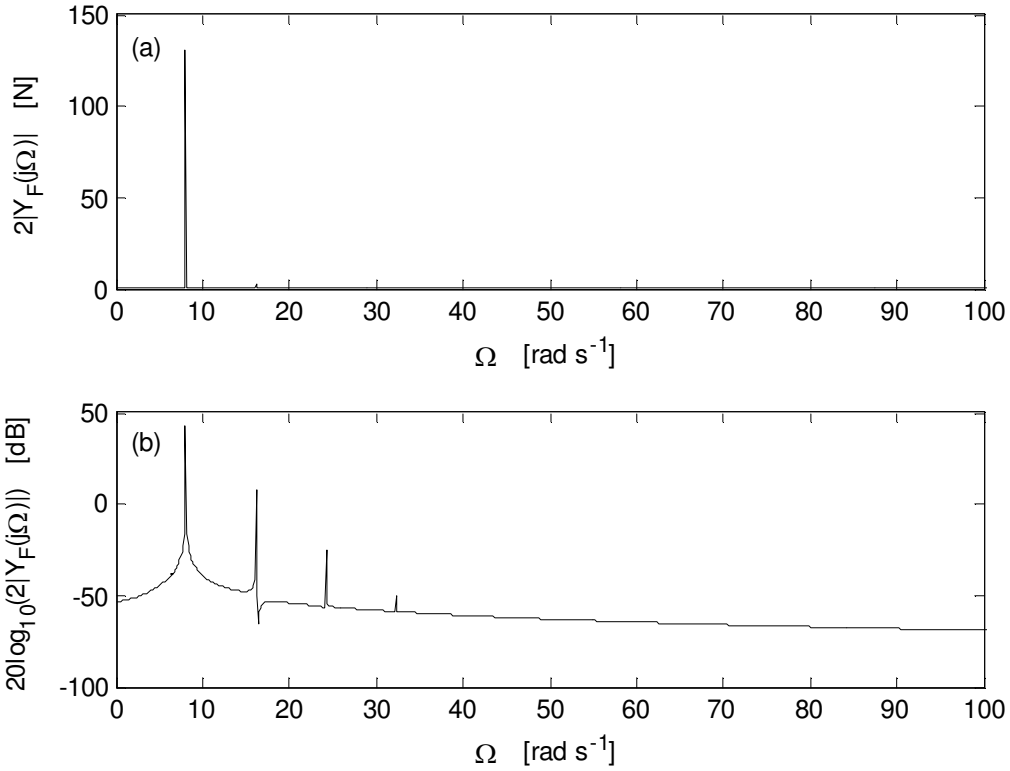

Fig. 7. The output frequency response when $f(\bullet) = a_1(\bullet) + a_2\left(10^{(\bullet)} - 1\right)$, $a_1 = 29.6$ s N m^{-1} and $a_2 = 1\times10^3$ s N m^{-1}: (a) Amplitude response, (b) Bode response.

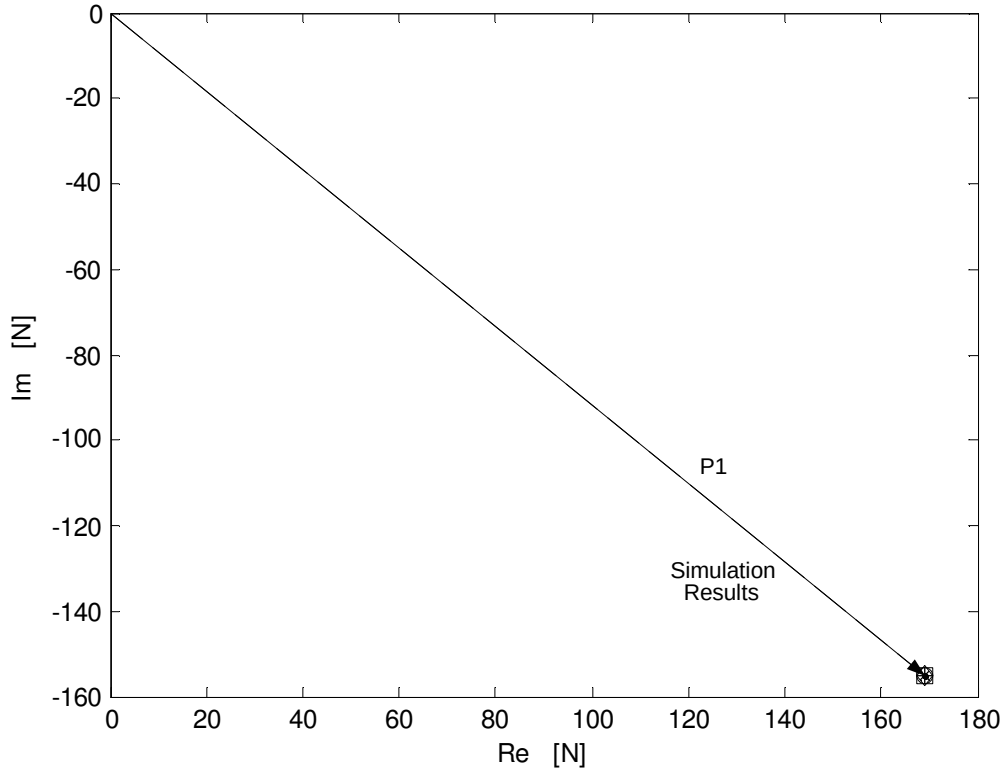

Fig. 8. The output frequency response $Y_F\left(j\Omega\right)$ at the driving frequency Ω when $f(\bullet)=a_1(\bullet)+a_3(\bullet)^3$, $a_1=29.6$ s N m^{-1} and $a_3=0$ s N m^{-1}. Solid lines: analytically determined results using nonlinear terms up to ninth order; dashed lines: simulation results.

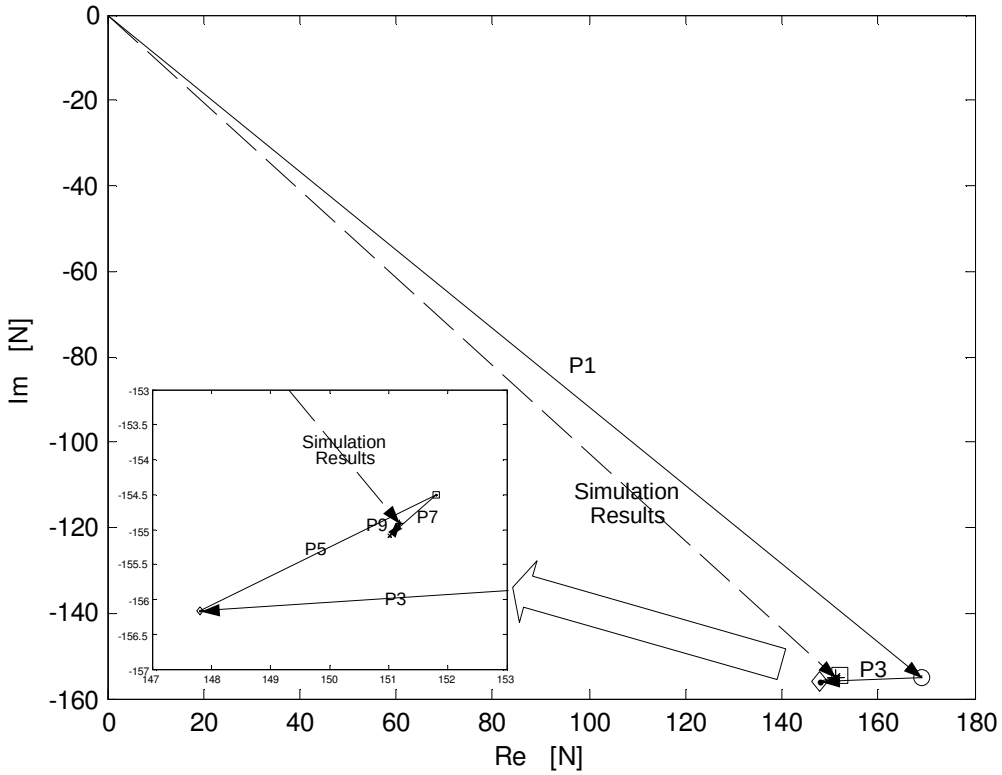

Fig. 9. The output frequency response $Y_F\left(j\Omega\right)$ at the driving frequency Ω when $f(\bullet)=a_1(\bullet)+a_3(\bullet)^3$, $a_1=29.6$ s N m^{-1} and $a_3=100$ s N m^{-1}. Solid lines: analytically determined results using nonlinear terms up to ninth order; dashed lines: simulation results.

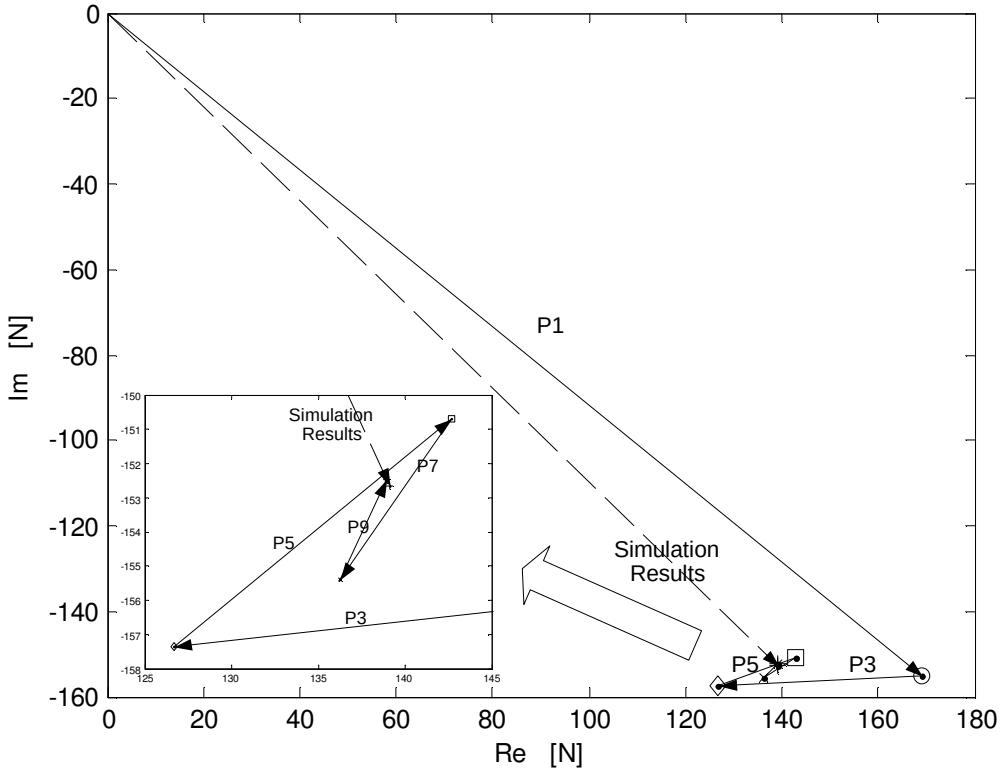

Fig. 10. The output frequency response $Y_F(j\Omega)$ at the driving frequency Ω when $f(\bullet) = a_1(\bullet) + a_3(\bullet)^3$, $a_1 = 29.6$ s N m^{-1} and $a_3 = 200$ s N m^{-1}. Solid lines: analytically determined results using nonlinear terms up to ninth order; dashed lines: simulation results.

Colour versions of selected figures

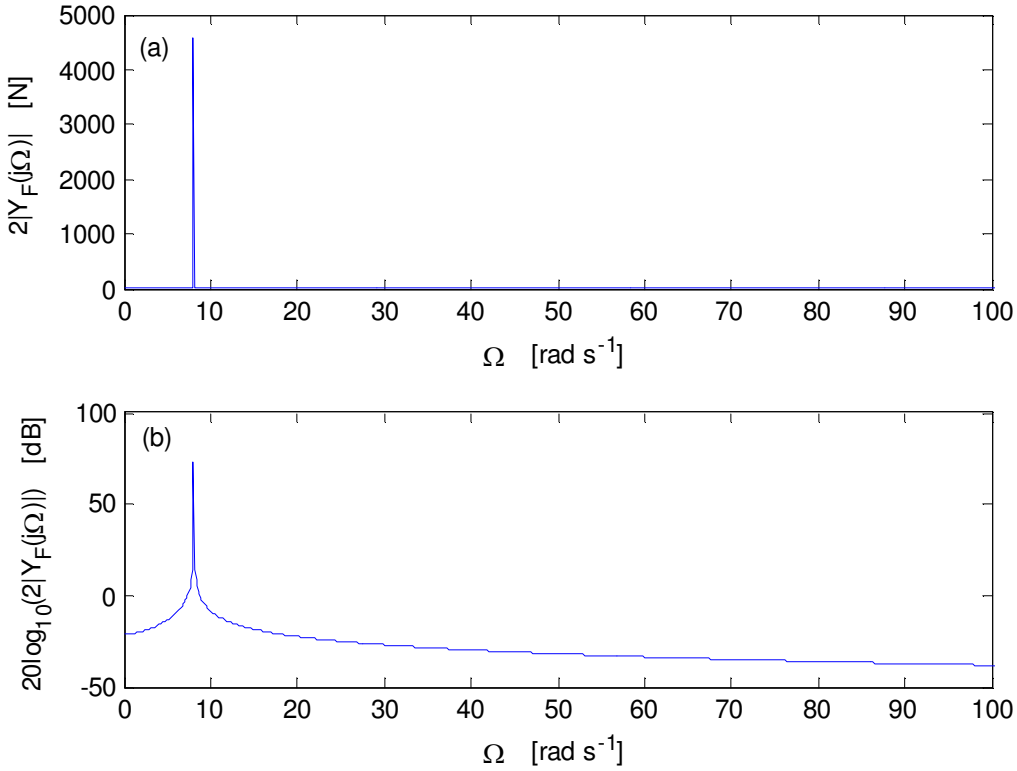

Fig. 2. The output frequency response when $f(\bullet) = a_1(\bullet) + a_3(\bullet)^3$, $a_1 = 29.6$ s N m^{-1} and $a_3 = 0$ s N m^{-1}: (a) Amplitude response, (b) Bode response.

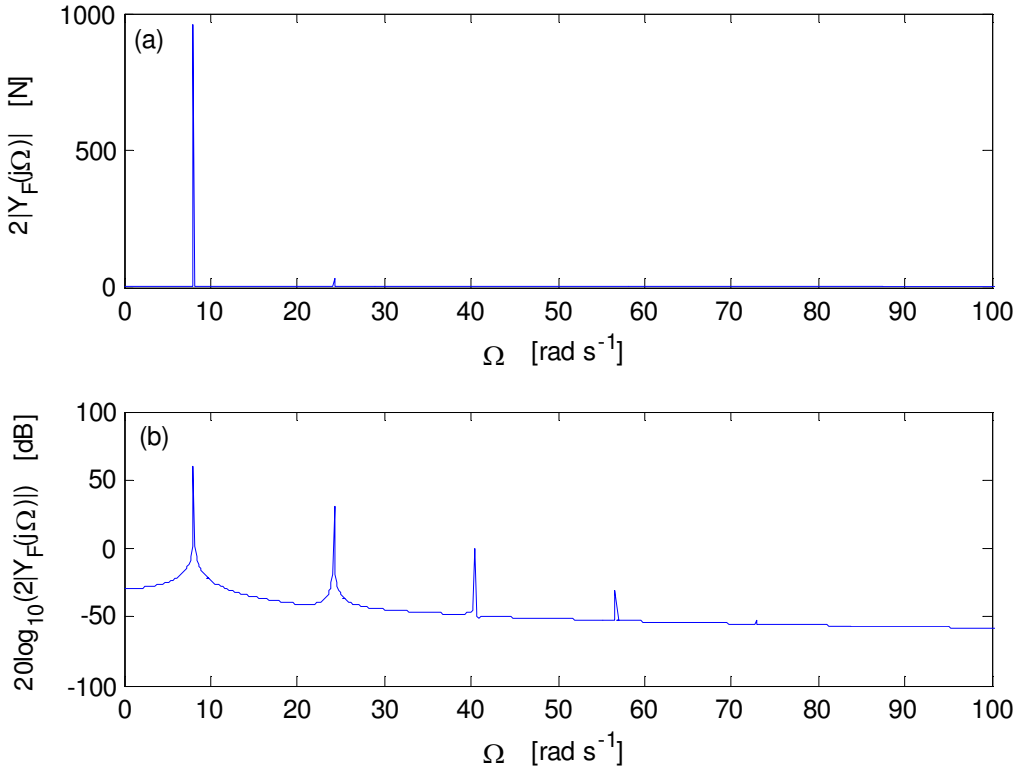

Fig. 3. The output frequency response when $f(\bullet) = a_1(\bullet) + a_3(\bullet)^3$, $a_1 = 29.6$ s N m^{-1} and

$a_3 = 1 \times 10^3$ s N m^{-1}: (a) Amplitude response, (b) Bode response.

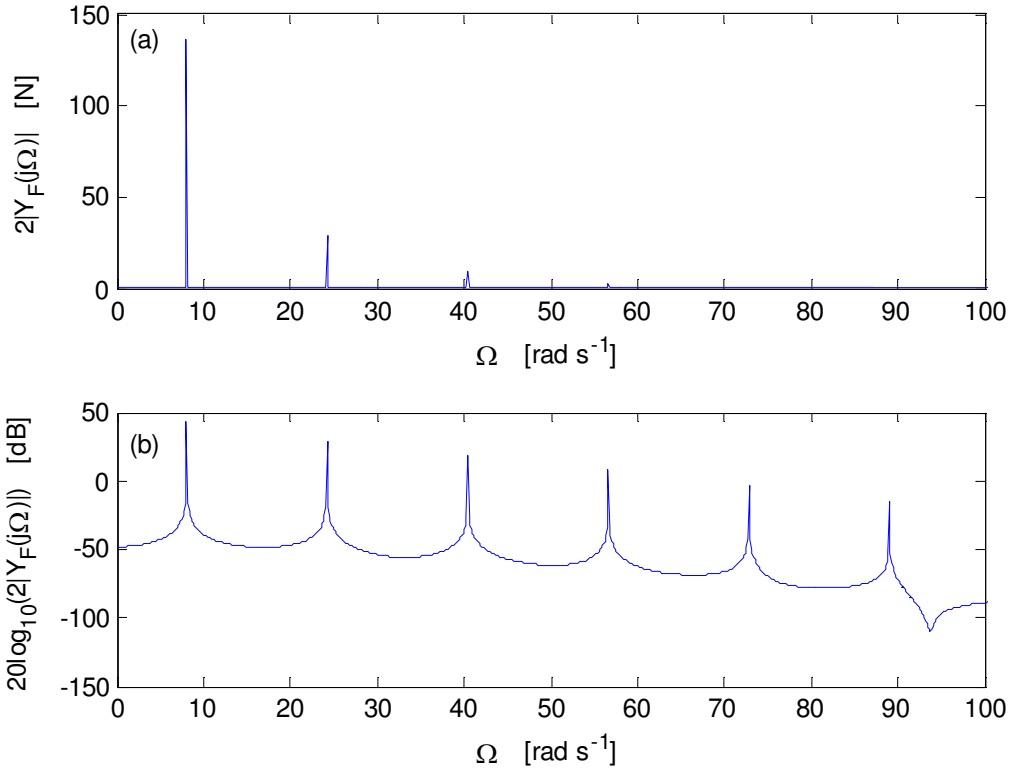

Fig. 4. The output frequency response when $f(\bullet) = a_1(\bullet) + a_3(\bullet)^3$, $a_1 = 29.6$ s N m^{-1} and $a_3 = 1 \times 10^6$ s N m^{-1}: (a) Amplitude response, (b) Bode response.

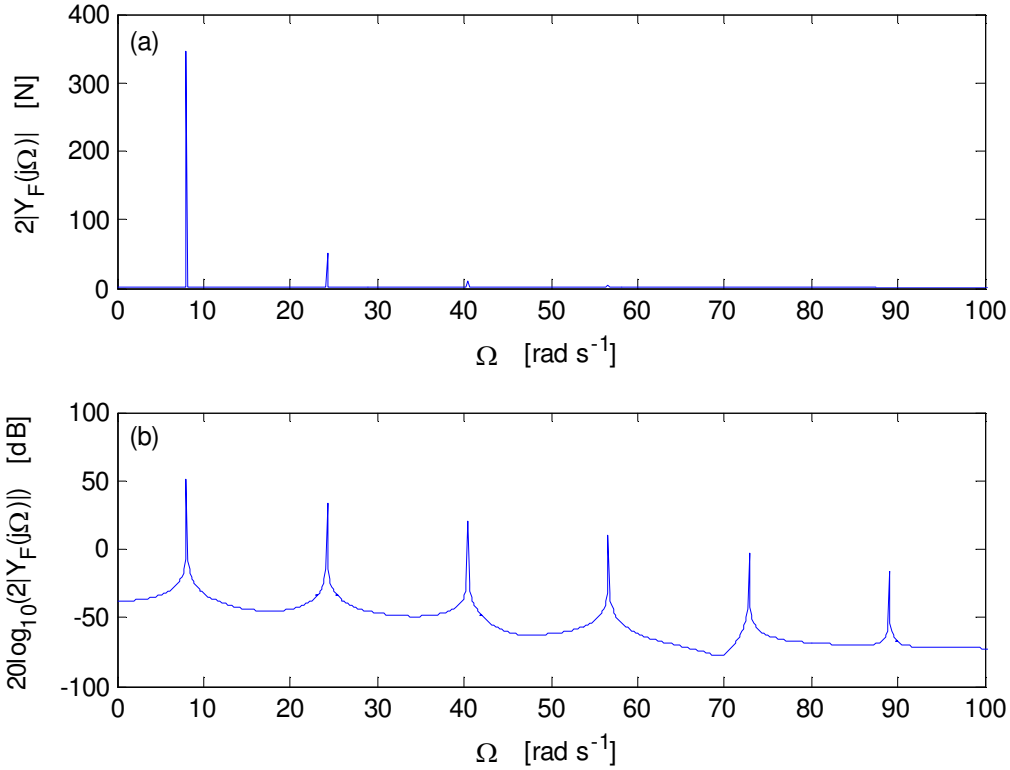

Fig. 5. The output frequency response when $f(\bullet) = a_1(\bullet) + a_3(\bullet)^3 + a_5(\bullet)^5$, $a_1 = 29.6$ s N m^{-1}, $a_3 = 1 \times 10^3$ s N m^{-1} and $a_5 = 1 \times 10^6$ s N m^{-1}: (a) Amplitude response, (b) Bode response.

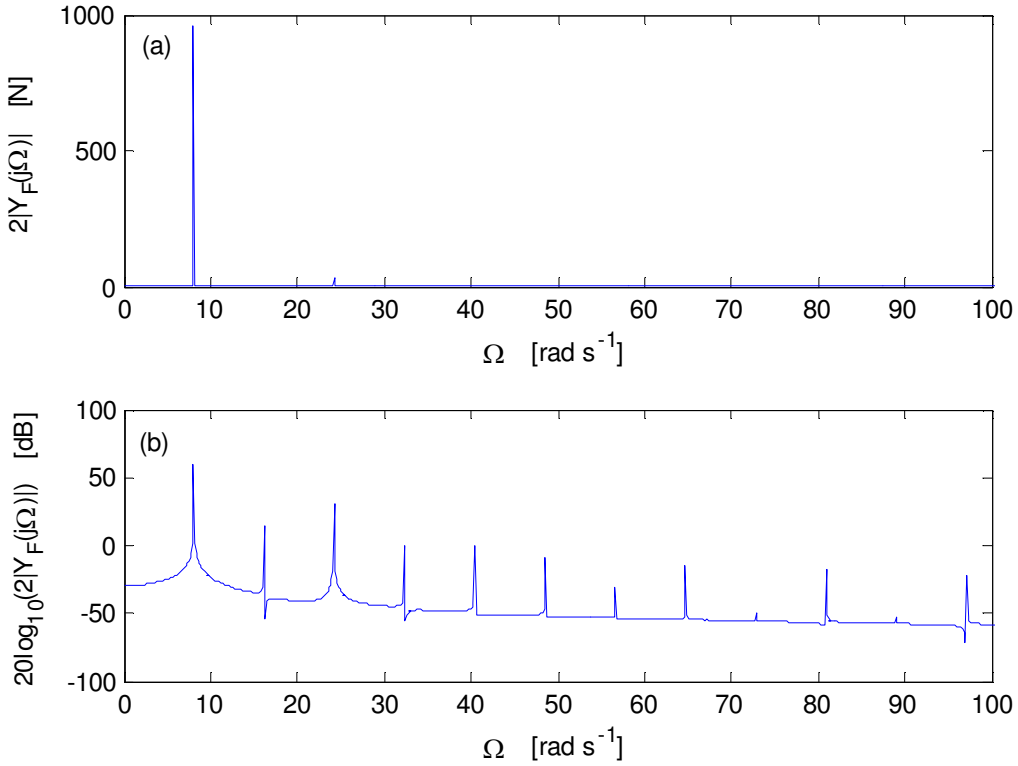

Fig. 6. The output frequency response when $f(\bullet) = a_1(\bullet) + a_2 |(\bullet)| + a_3(\bullet)^3$, $a_1 = 29.6$ s N m^{-1}, $a_2 = 20$ s N m^{-1} and $a_3 = 1 \times 10^3$ s N m^{-1}: (a) Amplitude response, (b) Bode response.

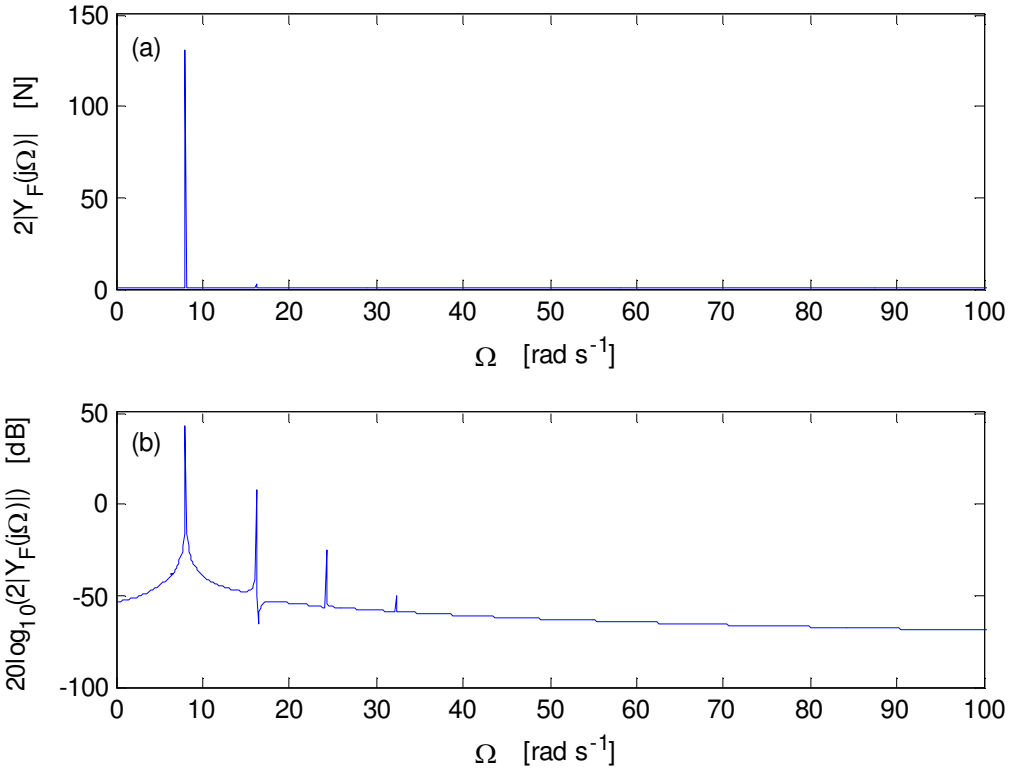

Fig. 7. The output frequency response when $f(\bullet) = a_1(\bullet) + a_2\left(10^{(\bullet)} - 1\right)$, $a_1 = 29.6$ s N m^{-1} and $a_2 = 1\times10^3$ s N m^{-1}: (a) Amplitude response, (b) Bode response.

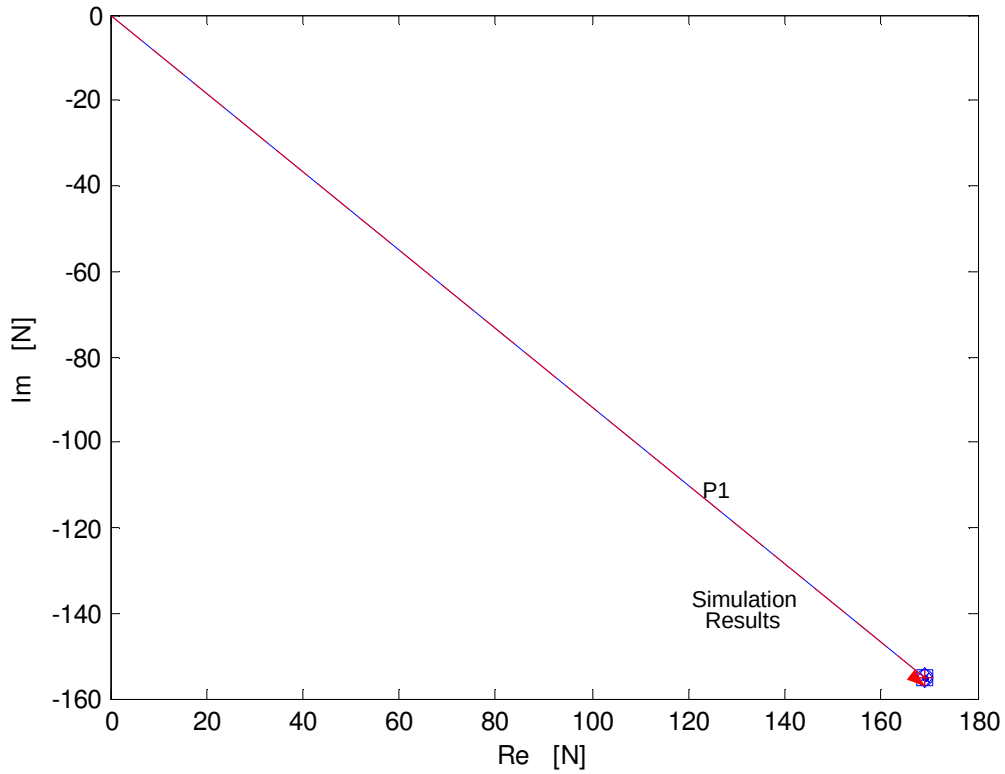

Fig. 8. The output frequency response $Y_F\left(j\Omega\right)$ at the driving frequency Ω when $f(\bullet)=a_1(\bullet)+a_3(\bullet)^3$, $a_1=29.6$ s N m^{-1} and $a_3=0$ s N m^{-1}. Solid lines: analytically determined results using nonlinear terms up to ninth order; dashed lines: simulation results.

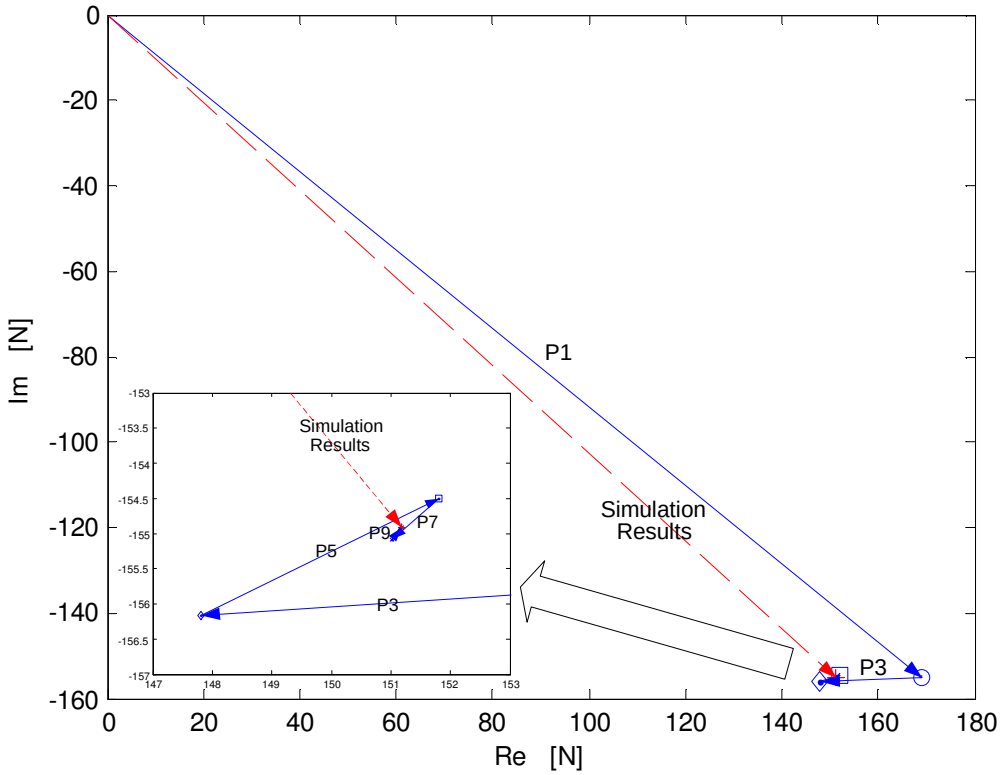

Fig. 9. The output frequency response $Y_F\left(j\Omega\right)$ at the driving frequency Ω when $f(\bullet)=a_1(\bullet)+a_3(\bullet)^3$, $a_1=29.6$ s N m^{-1} and $a_3=100$ s N m^{-1}. Solid lines: analytically determined results using nonlinear terms up to ninth order; dashed lines: simulation results.

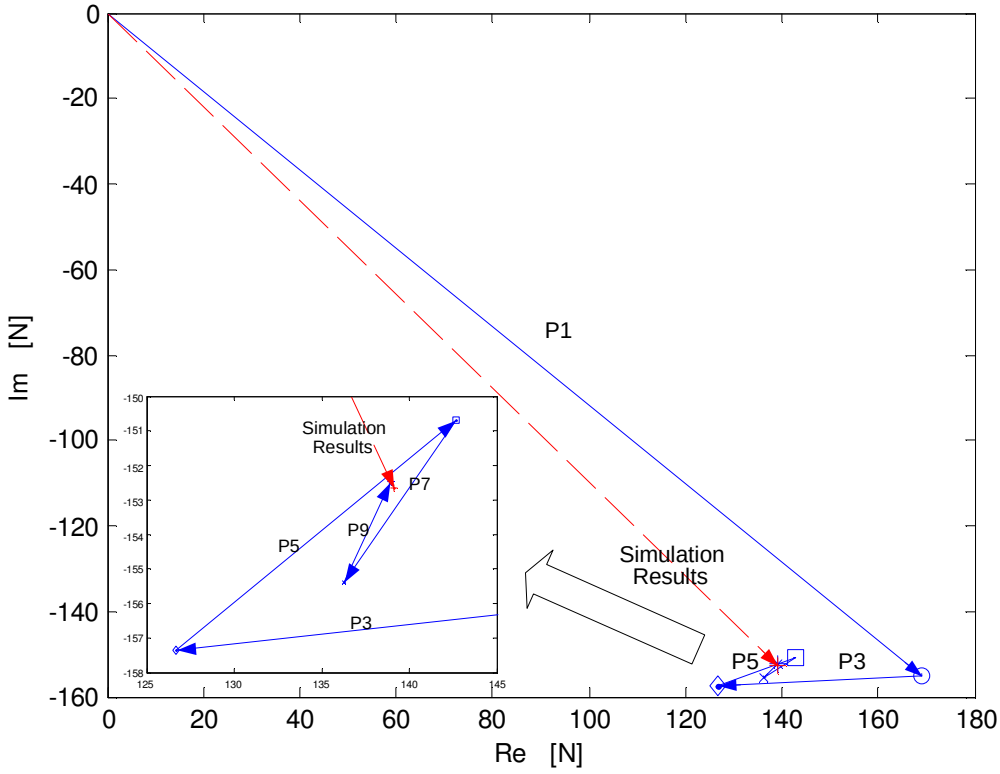

Fig. 10. The output frequency response $Y_F(j\Omega)$ at the driving frequency Ω when $f(\bullet) = a_1(\bullet) + a_3(\bullet)^3$, $a_1 = 29.6$ s N m^{-1} and $a_3 = 200$ s N m^{-1}. Solid lines: analytically determined results using nonlinear terms up to ninth order; dashed lines: simulation results.